# 7 Observation results

## 7.5 Effects of atmospheric variability on KSP geodetic network -Preliminary results-

by

Ichikawa Ryuichi, Yasuhiro Koyama and Yukio Takahashi

(recived on )

Running Title: 7.5 Effects of atmospheric variability

## Abstract

We applied the anisotropic mapping function for the purpose of examining an impact on the analyses of KSP/VLBI. The repeatability of horizontal coordinate within 5-days campaign measurements is significantly improved using the anisotropic mapping function. Estimated gradient vectors are consistent with synoptic scale gradient of water vapor retrieved from both nationwide GPS array of GSI and numerical weather prediction model of JMA. On the other hand, gradient vectors are incorrectly estimated, when the meso-scale phenomena such as the tropical depression occurs. Further quantitative evaluation is required to understand the space-time variability of water vapor and to improve repeatability of site coordinates using VLBI and GPS.

(Keywords: GPS, mapping function, tropospheric delay, VLBI)

## 1. Introduction

Tropospheric delay significantly degrades the precision of the Global Positioning System (GPS) and Very Long Baseline Interferometry (VLBI). One of the most crucial problems is the difficulty of the accurate vertical positioning. At present, observations at lower elevation angles are recommended to improve vertical accuracy. However, the advantage of this procedure is likely impaired by the azimuthal asymmetry of the delay due to meso-scale perturbation. Meso-scale phenomena such as heavy rainfall, land and sea breezes, and severe storms frequently occur in the Kanto district of Japan, where the Key Stone Project (KSP) geodetic network is located. Recently, several anisotropic mapping functions [(1)(2)] in which atmospheric gradients are assumed to have a simple linear form have been proposed. The MacMillan gradient model is available in the VLBI analysis software. It is very important to evaluate the efficiency of the atmospheric gradient model in the VLBI analysis of KSP. We will report the preliminary results of VLBI analysis using the gradient model.

## 2. Data analysis

In the KSP network the experimental observation from July 27 through August 1, 1997 was carried out as a research and development experiment of KSP. Four KSP sites (Kashima, Koganei, Miura, and Tateyama) are equipped with VLBI facilities, geodetic GPS receivers, and surface meteorological equipment. Ashtech Z-XII GPS receivers observed for 24 hours each day at 30-second intervals all GPS satellites with elevation angles above 5 degrees. The VLBI facilities did likewise observed for 24 hours each day at a minimum elevation angle of 10 degrees. The VLBI and GPS systems of KSP are described in detail in another paper [3][4].

VLBI data were analyzed with SOLVE (Ver. 5.0094) and CALC (Ver. 8.2) software[5]. GPS data were analyzed with Bernese Ver. 4.0 software [6] using precise satellite orbits generated by the Center for Orbit Determination (CODE) in Berne, Switzerland. In the analyses of VLBI and GPS, geodetic station coordinates were estimated for Koganei, Miura, and Tateyama sites relative to Kashima site. Tropospheric delays in the zenith direction were simultaneously estimated every three hours. Elevation angle cutoff values are changed for 5 (only GPS analysis), 10, 15, and 20 degrees in order to investigate elevation-dependent systematic errors, such as mapping function errors.

Since these software include an atmospheric gradient option, we have applied the gradient model in the analysis of VLBI data at the minimum elevation angle of 10 degrees. We tried to estimate the gradient vector parameters for each KSP site. However, it was difficult to estimate the parameters accurately because of the instability of the least squares estimation due to the relatively short baseline length of less than 150 km. Thus, we estimated the gradient vector parameters for only the Tateyama site, though the estimated parameters include the effects of the atmospheric gradient at the other three sites. Unfortunately, the gradient estimation option is unavailable in the Bernese Ver. 4.0.

## 3. Results and discussion

Figure 1 shows the time series of the daily three-dimensional position of the Tateyama site with respect to the Kashima site from July 28 through August 1, 1997. Both GPS and VLBI solutions for all components show similar characteristics. For example, the north components are moving to the north on July 28 thru 30 and are moving to the south from July 31 thru August 1. East components are moving to the east from July 30 thru August 1. In particular, Fig. 1 shows that the east components estimated by VLBI on July 28 and 30 are moving toward the west at a lower elevation cutoff angle. We suggest from these results that some systematic effects such as the atmospheric gradient are causing daily variations in the site coordinates.

In Fig. 1 we also show the VLBI estimates of the position with and without atmospheric gradient parameters at the minimum elevation of 10 degrees. When gradients are estimated with a 10-degree elevation cutoff, the RMS of the north component is reduced from 5.0 mm to 4.2 mm and the RMS of the east component is reduced from 5.0 mm to 2.1 mm. Moreover, the RMS of the vertical component is slightly increased from 15.7 mm to 15.8 mm. Improvements for the north and east components are significant from July 28 thru July 30. The westward drifts of VLBI solutions at lower elevation cutoff angles as shown in Fig. 1 are recovered by estimating the atmospheric gradient.

We have to test whether the VLBI gradient estimates are physically reasonable. In Fig. 2 we show the estimates of the NS and EW gradient delays for the Tateyama site in the north and east directions, respectively. Since the estimated gradient vectors include the effects of the atmospheric gradient for all four sites, it is not easy to verify the effects of the atmospheric gradient at each site. Thus, we investigated the spatial variability of water vapor content in the Kanto district in order to get some insights on the atmospheric gradient. Figure 3 shows the zenith wet delay estimated by the permanent GPS array of the Geographical Survey Institute (GSI), and Fig. 4 shows the precipitable water vapor (PWV) values retrieved from the high-resolution (20-km grid intervals and 36 vertical levels) numerical prediction data of the Japan Meteorological Agency (JMA). The term of PWV is the length of an equivalent column of liquid water. The zenith wet delay is roughly 6.4 times the PWV in units of length[(7)].

Figures 3 and 4 show two significant characteristic variabilities of water vapor. One is the synoptic scale variation which has a north-south gradient and the other is the local-scale variations caused by tropical depression. On July 29 a north-south gradient was dominant according to Figs. 3 and 4. The gradient as shown in these figures is consistent with the improvement of the north component of the VLBI solution using the gradient estimation on that day. In contrast, the result on July 28 is affected by both a northeast gradient at Kashima (fixed site) and a north-south gradient at Tateyama. Since the north gradient is due to synoptic scale variation, the magnitude of the north component at the two sites is almost the same. Therefore, we infer from the images shown in Fig. 3 that the north components of the gradient vector at Kashima and Tateyama cancel each other out. As a result, we think that there is no clear improvement of the north component.

For a more detailed interpretation further investigations are required - comparisons with water vapor radiometer (WVR) data for example. WVR observations were started on June 24, 1998 and are still in progress. WVR observations are being collected at four stations. Two WVRs, one at the Meteorological Research Institute (MRI) of Tsukuba and one at the Communications Research Laboratory (CRL) of Kashima, are sequentially pointed towards each of the GPS satellites in view. Another two WVRs, one at the GSI of Tsukuba and one at Chiba University, are sequentially pointed from north to south at elevations of 10, 15, 30, 45, 75 and 90 degrees. Our main concerns are (1) What is the dominant scale of disturbances causing significant positioning errors? (2) Are anisotropic mapping functions sufficient for removing the effects of meso-scale and local scale disturbances? (3) Is it possible and useful to develop a new method for the correction of GPS and VLBI using a Numerical Weather Prediction (NWP) Model? The results of the WVR observations will be reported in another paper.

## 4. Concluding remarks

The anisotropic mapping functions are preliminarily applied examining their impact on the analyses of experimental measurements of KSP/VLBI. The 5-day repeatability of the horizontal coordinate is significantly improved using the anisotropic mapping function. Estimated gradient vectors are consistent with synoptic scale gradient of water vapor retrieved from the nationwide GPS array of GSI and numerical weather prediction model of JMA. Gradient vectors are incorrectly estimated, however, when the meso-scale phenomena such as the tropical depression occurs. Therefore, we have to quantitatively evaluate the space-time variability of water vapor under the various meteorological conditions. For this purpose, we have been carrying out an experimental measurement for detecting and characterizing variations in water vapor by using water vapor radiometers (WVRs) in the Kanto district of central Japan.

## Acknowledgments

We thank Dr. N. Mannoji for providing the Japan Analysis data sets of the Japan Meteorological Agency. We used zenith wet delay data estimated by GPS array of the Geographical Survey Institute.

## References

(1) MacMillan, D.S., "Atmospheric gradients from very long baseline interferometry observations", Geophys. Res. Lett., 22, 1041-1044, 1995.

(2) Chen, G. and T. A. Herring, "Effects of atmospheric azimuthal asymmetry on the analysis of space geodetic data", J. Geophys. Res., 102, 20489-20502, 1997.

(3) Koyama, Y., T. Iwata, and H. Takaba, "Observation and System Management Software", J. Comm. Res. Lab., this issue, 1999.

(4) Ichikawa, R., "GPS system of KSP geodetic network", J. Comm. Res. Lab., this issue, 1999.

(5) C. Ma, J. W. Ryan and D. S. Caprette, “NASA Space Geodesy Program-GSFC Data Analysis-1993, VLBI Geodetic Results 1979-92”, NASA TM-104605, Goddard Space Flight Center, 1994.

(6) Rothacher, M. and L. Mervart (eds.), “Bernese GPS Software Version 4.0”, 418 pages, Astronomical Institute, University of Bern, 1996.

(7) Hogg, D. C., F. O. Guiraud, and M. T. Decker, “Measurement of excess radio transmission length on earth-space paths”, Astron. Astrophys., 95, 304-307, 1981.

## Figure captions

**Fig. 1** Estimates of the north, east, and vertical components of the Tateyama site relative to the Kashima site from July 28 - August 1 1997.

**Fig. 2** Gradient component estimates from VLBI at the Tateyama site. The estimated piecewise-linear gradient functions with two-hour intervals are shown for the north and east components.

**Fig. 3** Zenith wet delay images retrieved from the GSI GPS array from 0000UT July 28 - 1800UT July 30, 1997 (6-hour intervals). Contour interval is 1 cm.

**Fig. 4** Images of precipitable water vapor retrieved from the high-resolution numerical prediction data of the Japan Meteorological Agency from 0000UT July 28 - 1200UT July 30, 1997 (12-hour intervals). Contour interval is 0.25 cm.

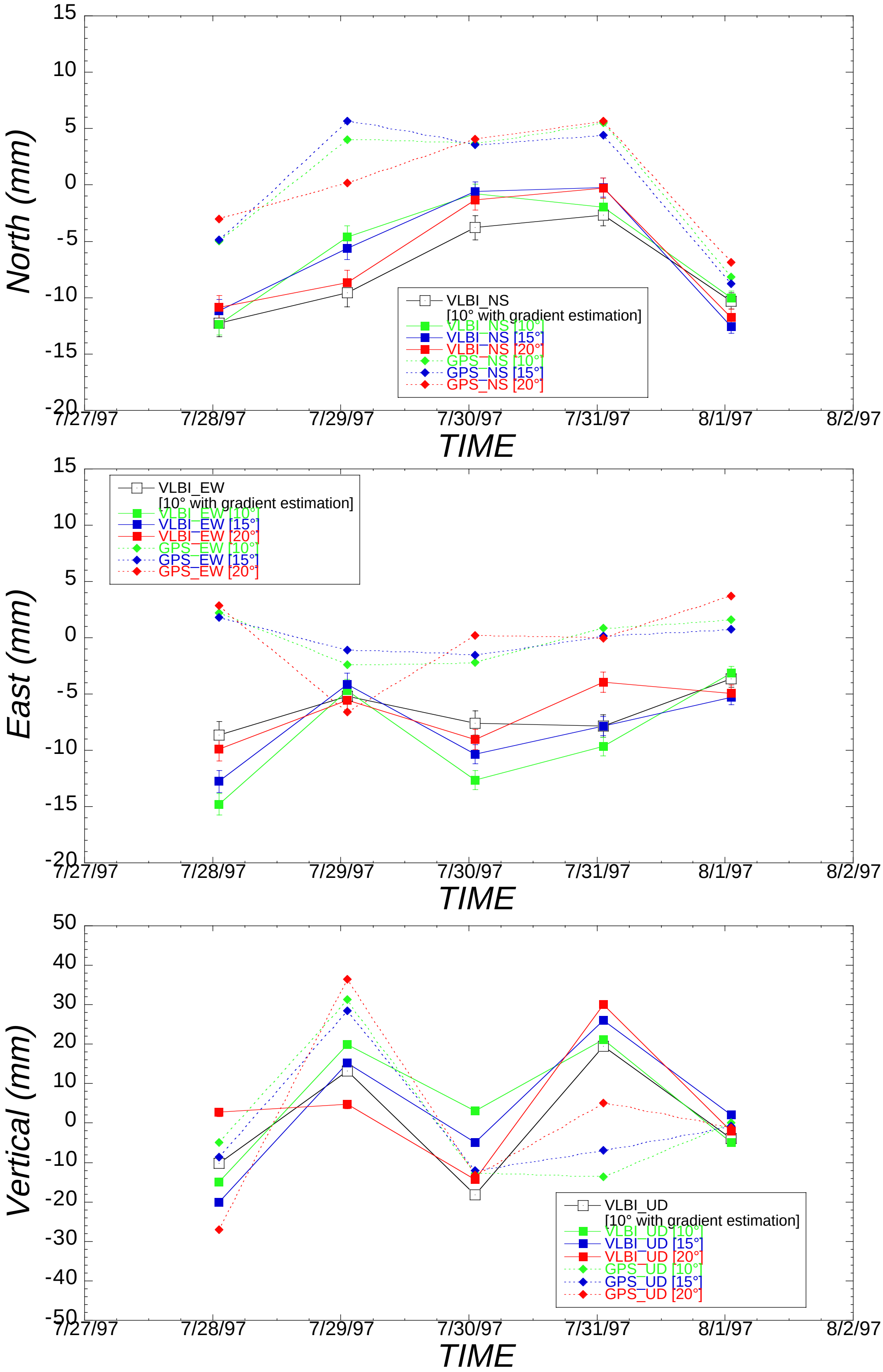
North (mm)
East (mm)
Vertical (mm)
TIME
7/27/97
7/28/97
7/29/97
7/30/97
7/31/97
8/1/97
8/2/97
VLBI_NS
[10° with gradient estimation]
VLBI_NS [10°]
VLBI_NS [15°]
VLBI_NS [20°]
GPS_NS [10°]
GPS_NS [15°]
GPS_NS [20°]
VLBI_EW
[10° with gradient estimation]
VLBI_EW [10°]
VLBI_EW [15°]
VLBI_EW [20°]
GPS_EW [10°]
GPS_EW [15°]
GPS_EW [20°]
VLBI_UD
[10° with gradient estimation]
VLBI_UD [10°]
VLBI_UD [15°]
VLBI_UD [20°]
GPS_UD [10°]
GPS_UD [15°]
GPS_UD [20°]

Fig. 1

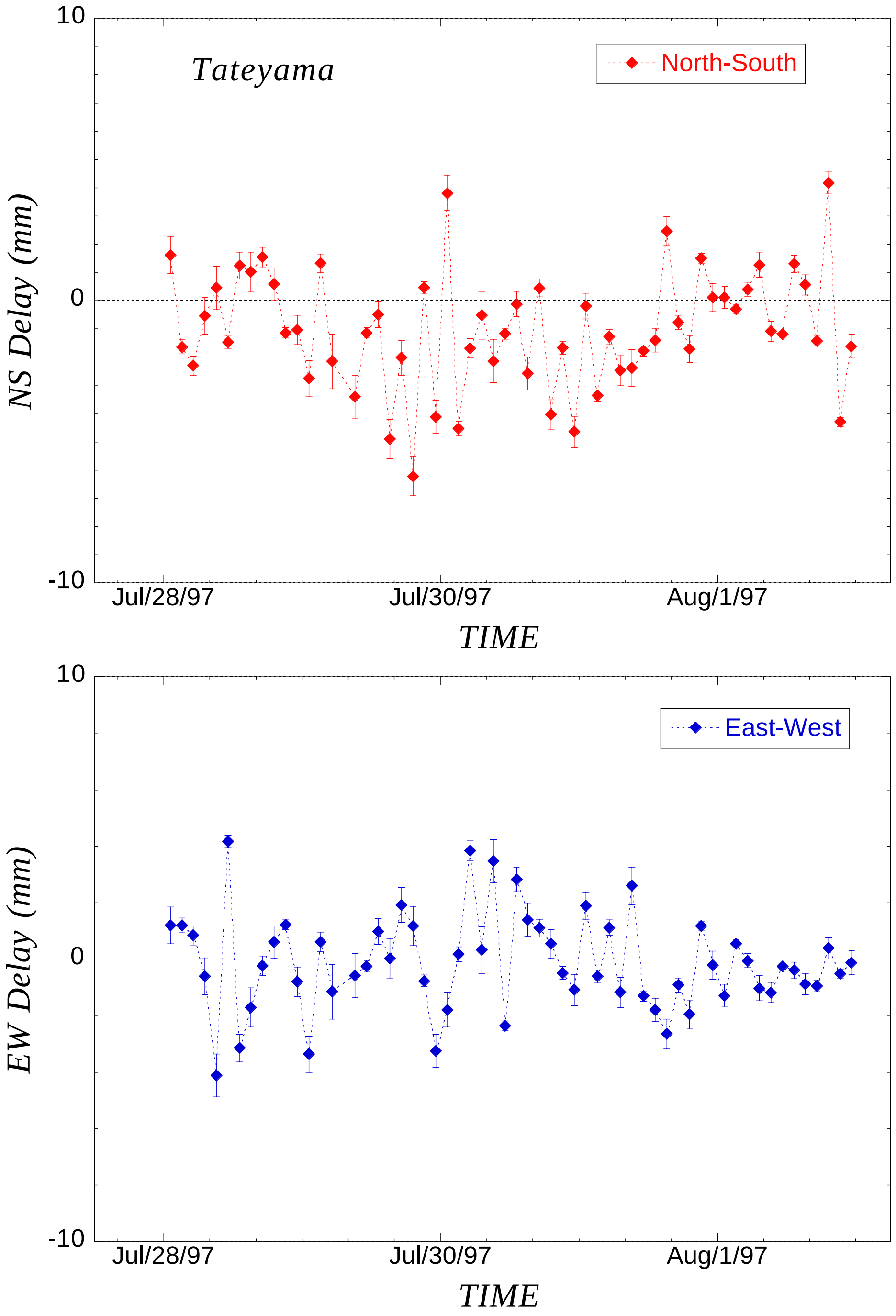
Tateyama
North-South
NS Delay (mm)
10
0
-10
Jul/28/97
Jul/30/97
Aug/1/97
TIME
East-West
EW Delay (mm)
10
0
-10
Jul/28/97
Jul/30/97
Aug/1/97
TIME

Fig. 2

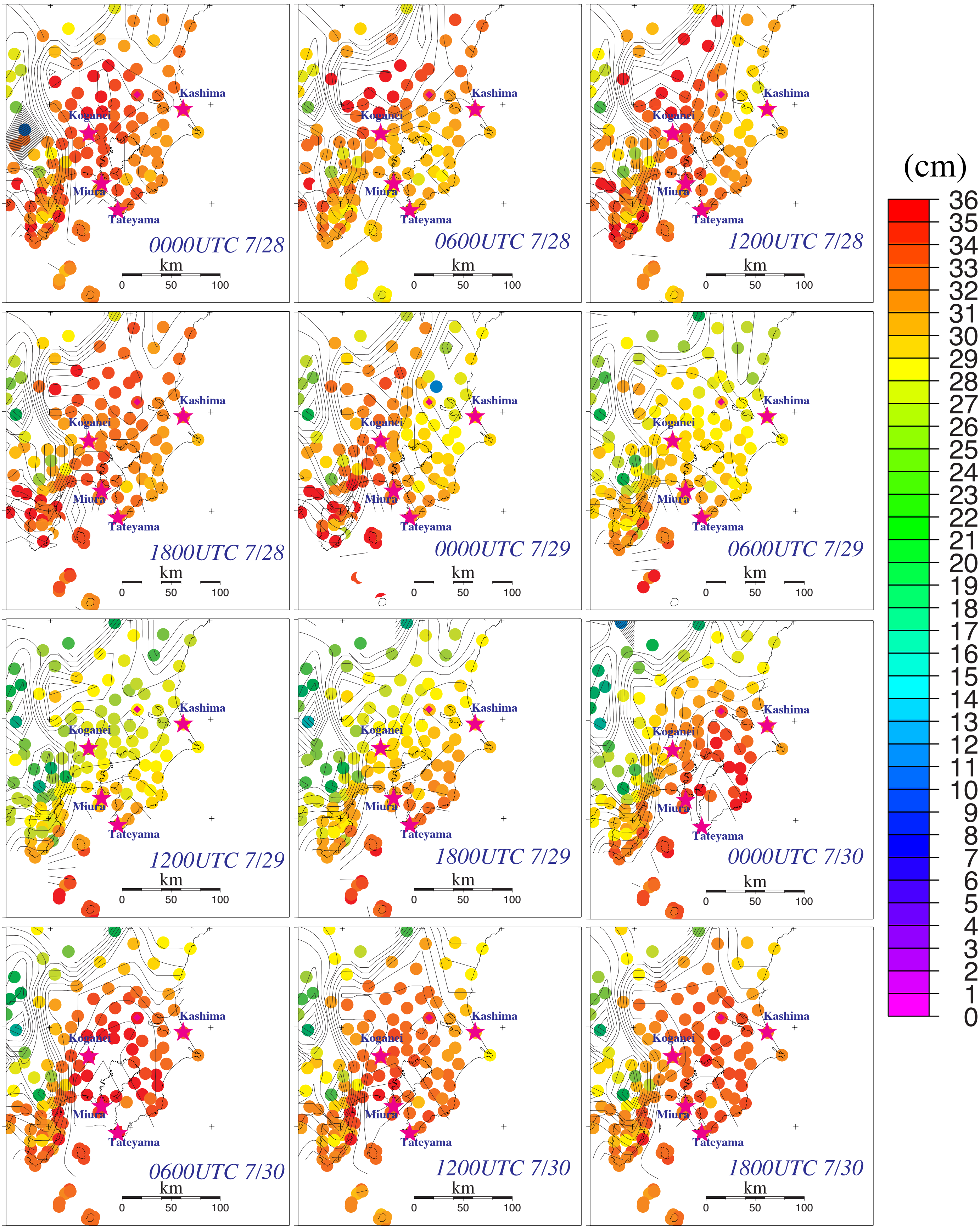

Kashima
Koganei
Miura
Tateyama
0000UTC 7/28
0600UTC 7/28
1200UTC 7/28
1800UTC 7/28
0000UTC 7/29
0600UTC 7/29
1200UTC 7/29
1800UTC 7/29
0000UTC 7/30
0600UTC 7/30
1200UTC 7/30
1800UTC 7/30
km
0 50 100
(cm)
36 35 34 33 32 31 30 29 28 27 26 25 24 23 22 21 20 19 18 17 16 15 14 13 12 11 10 9 8 7 6 5 4 3 2 1 0


Fig. 3

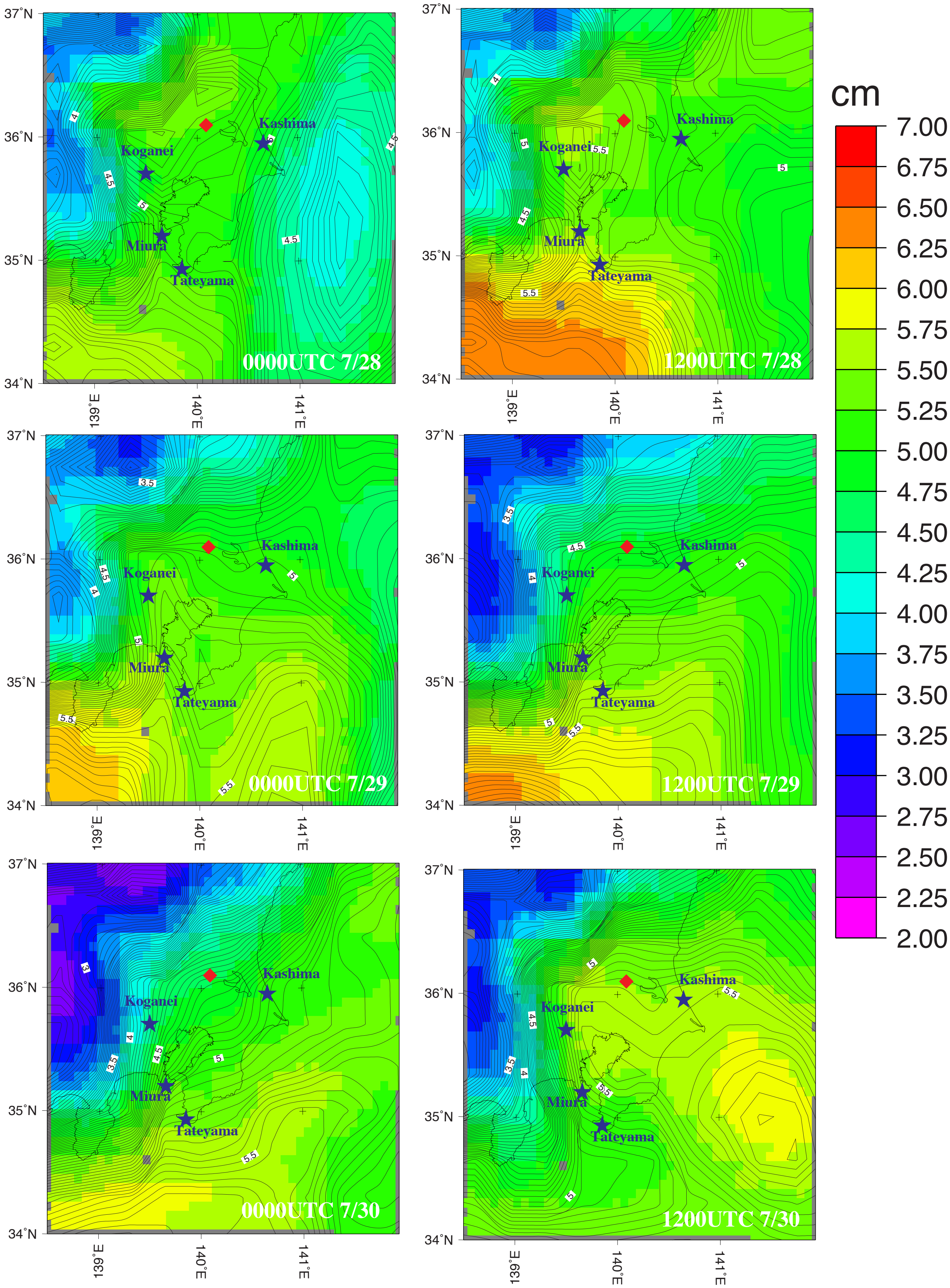
0000UTC 7/28
1200UTC 7/28
0000UTC 7/29
1200UTC 7/29
0000UTC 7/30
1200UTC 7/30
Kashima
Koganei
Miura
Tateyama
37°N
36°N
35°N
34°N
139°E
140°E
141°E
cm
7.00
6.75
6.50
6.25
6.00
5.75
5.50
5.25
5.00
4.75
4.50
4.25
4.00
3.75
3.50
3.25
3.00
2.75
2.50
2.25
2.00

# Fig. 4